Journal of Applied Research and Technology

www.jart.icat.unam.mx

ICAT Instituto de Ciencias Aplicadas y Tecnología

Journal of Applied Research and Technology 22 (2024) 266-273

Original

Effect of blade materials on the undershot water turbine performance

E. Yohanes Setyawan[a]* • D. Hari Praswanto[a] • S. Bahri L. M[b]

[a]*National Institute of Technology Malang. Malang, Indonesia*
[b]*Khairun University. Ternate, Indonesia*

Received 05 27 2021; accepted 03 18 2022
Available 04 30 2024

Abstract: Undershot waterwheel at low flow with an average discharge of 0.12 m3/s and 613.2 W water horsepower are used to turn the waterwheel. The rotation results obtained with aluminum material is 24 RPM which has a density of 2.71 g/cm3 while the lowest rotation is owned by a galvanic of 20 RPM with a density of 7.49 g/cm3. From the experiment, it was found that the difference between the materials used was due to the different densities. The efficiency of waterwheels with aluminum material has the highest value, namely 30%, while the lowest using acrylic material has an efficiency of 23%. The highest generator efficiency uses aluminum material with an efficiency of 4.2%, and the second has an efficiency of 3.6% using aluminum composite panel material. Aluminum has the highest efficiency because it has less density than galvanized. In addition, the thickness of aluminum is also very influential, where aluminum has a thickness of 1.14 mm while galvanized has 0.98 mm.

Keywords: Waterwheel, undershot, aluminum, galvanized, density

*Corresponding author.
E-mail address: yohanes@lecturer.itn.ac.id (E. Yohanes Setyawan).
Peer Review under the responsibility of Universidad Nacional Autónoma de México.

1. Introduction

The issue of energy nowadays is a crucial point of some rules that have been made by the government, especially regarding energy needs because many areas have not been electrified. There are also rules regarding alternative energy as a solution for the development of future energy that is currently being developed (Panwar et al., 2011; Yuksek et al., 2006). One of them is hydropower as it exploits underutilized resources such as rivers or small streams (Rohmer et al., 2016; Setyawan et al., 2020). Indonesia itself has a lot of potential energy sources that can be utilized, such as solar energy, which is always available throughout the year. Therefore, modern designs are developed using solar that is used with optimal performance (Suravut et al., 2017). The energy potential of the river flow is very promising as it can be utilized as much as possible to produce electrical energy (Yükse et al., 2008; Yukse, 2010). Potential energy from small river fluid flow or irrigation can be extracted into electricity (Nuramal et al., 2017). It is expected that the potential of river flow in Indonesia can be utilized to the maximum extent possible to be converted into electrical energy so that it no longer experiences a shortage of electrical energy needs. There are many streams in several areas such as Java, Sumatra, Kalimantan, and Papua, and many more in other islands that can be utilized. The urgent need is making waterwheels using easy-to-found materials such as wood materials that have low efficiency (Vashisht, 2012; Williamson et al., 2014) as it is done traditionally. To increase efficiency even greater, vertical-type waterwheels that consider the density of the material used can be made (Denny, 2004; Müller & Kauppert, 2004). The mass of the material is very influential on the change in potential energy present in the flow of water into mechanical energy as the rotation of the water wheel used to turn the generator to produce electrical energy (Adanta et al., 2020).

Prasad et al. (2009) compared the axial efficiency of flow turbines coming through experimental and CFD analysis with three different guide vane angles. Whereas Jain et al. (2010) conducted a study of the performance and efficiency of a French turbine in four different operations at the propeller point by using CFD and to validate the same as evaluating the model. (Kim et al., 2009), analyzed the performance of water turbines by varying the effect of tangential and axial pressures, which examined the velocity distribution on turbine performance using CFD (Setyawan et al., 2017). The purpose is to get the maximum development of hydropower turbines in industrial activities (Viollet, 2017). Hung also analyzed the performance and field of the waterwheel by utilizing tidal energy by using six and nine blades resulting in more blades that used greater torque (Nguyen et al., 2018). Water energy can be utilized and used in the form of mechanical energy to produce electrical energy using simple equipment, most of which are around us (Agar et al., 2008). The average waterwheels are used on a small scale so precise calculations are needed to get maximum results such as the use of composite materials (Wang et al., 2012).

Waterwheels are expected to evolve into an efficient tool that can be used at any time, of course using design and analysis that uses several important parameters to improve its efficiency (Denny, 2004; Sritram & Suntivarakorn, 2017).

Ishola has conducted research on hydroelectric power for additional power storage using three types of suitable materials steel, A390 cast aluminum alloy, and plastics (Ishola et al., 2019). The research was conducted to study the effect of turbine materials on the efficiency of power generation from hydroelectric plants made of steel and aluminum. The results showed that the maximum power generation efficiency of steel and aluminum turbines is 33.56% and 34.79% and that the efficiency of aluminum turbines is higher than that of steel turbines on average 8.4% and 8.14%, respectively. These results suggested that a lighter water turbine can improve torque and efficiency (Sritram et al., 2015). Previous research that has been conducted by Setyawan was the design of waterwheels with designs to meet small-scale power consumption, especially for household consumers in areas far from the city using undershot waterwheels with twelve blades (Setyawan et al., 2019). From several analyses from the results of previous research, in the analysis aiming to get the appropriate material, to get maximum efficiency, four materials were chosen to be used for waterwheel blades, namely aluminum, galvanized, acrylic, and aluminum composite panels.

2. Method

The design of the waterwheel is based on theory and several approaches to get good efficiency, and the theoretical approach of a flat plate that is placed in the water flow is used to rotate a waterwheel which consists of 12 blades with a 19 mm axle shaft. In this condition, velocity, force, and equation were used below. As shown in Figure 1 (Kumara, 2014)

$$S=L \times (D/2) \times (1-\cos\boldsymbol{\theta}/\sin\boldsymbol{\alpha}) \quad (1)$$

S is the submerged surface of the blade where L is the width of the water wheel (m), D is the diameter of the water wheel (m) and α is the angle of inclination.

$$P=Cp \times (\boldsymbol{\rho}/2) \times vr^2 \times S \quad (2)$$

P is the lift; Cp is the lift coefficient; ρ is the density (kg/m^3); Vr is the radial velocity (m/s); S is the submerged blade surface (m).

$$R=Cp \times (\rho/2) \times vt^2 \times S \quad (3)$$

The tensile force where *Cp* is the coefficient of lift ρ is the density (kg/m^3); *Vt* is the tangential velocity (m/s); *S* is the submerged blade surface (m).

$$F = \sqrt{P^2 + R^2} \quad (4)$$

F is the resultant force.

$$Fu = F \times \cos \boldsymbol{\varepsilon} \quad (5)$$

$$\boldsymbol{\varepsilon} = \arctan (CR/CP) - (a - \boldsymbol{\gamma}) \quad (6)$$

Fu is the useful force and its angle, while $\boldsymbol{\gamma}$ is the angle of relative velocity. As shown in Figure 1.

$$M = Fu \times (D/4) \times (1+\cos\boldsymbol{\theta}/\sin \boldsymbol{\alpha}) \quad (7)$$

M is the useful moment, while $\boldsymbol{\theta}$ is the angle between the center of the wheel and the maximum load position of the blade.

$$Nu = M \times \boldsymbol{\omega} = Fu \times vt \quad (8)$$

$$Nmed = Ki\ S(Nu/n) \quad (9)$$

Nu is the instantaneous force and the average force where *n* is the number of points calculated between the zero action positions. The value usually taken is between 1 <n <6 and the maximum load position of the blade, whereas *Ki* is the active blade coefficient, for the undershot type of turbine *Ki* = 1, 6.

$$Nmax = (\boldsymbol{\rho}/2) \times S\ max \times vam^3 \quad (10)$$

$$Smax = L \quad (11)$$

Nmax is the maximum force of flow, *Smax* is the maximum surface of the blade submerged and *h* is the ratio of blade submerged.

$$\boldsymbol{\eta} = Nmed / Nmax \quad (12)$$

$\boldsymbol{\eta}$ is the efficiency of the water wheel. Whereas $\boldsymbol{\omega}$ is angular velocity:

$$\boldsymbol{\omega} = 4vt / [D(1+ \cos\boldsymbol{\theta}/\sin \boldsymbol{\alpha})] \quad (13)$$

*n med*is the rotation speed:

$$n\ med = (30/\pi n) \times S\ \boldsymbol{\omega} j \quad (14)$$

$$\boldsymbol{\theta} = \cos\text{-}1[\{(0.5 \times D) - (B \times h)\}/ (0.5 \times D)] \quad (15)$$

$$\boldsymbol{\alpha} = (90 - \boldsymbol{\theta}) + \boldsymbol{\theta} \times (m / m+1) \quad (16)$$

*m*is a constant of 1≤m≤6.

To find out the Radial velocity, the following equation was used:

$$Vr = v(Vam^2 - 2 \times Vam \times Vt \times \sin a + Vt^2) \quad (17)$$

Tangential velocity equation used:

$$Vt = (Vam \times \sin \boldsymbol{\alpha}) \times 0.5 \times [1+(\cos\boldsymbol{\theta}/\sin \boldsymbol{\alpha} \quad (18)$$

$$\tan \boldsymbol{\gamma} = (Vt \times \cos a) / (Vam - Vt \times \sin a) \quad (19)$$

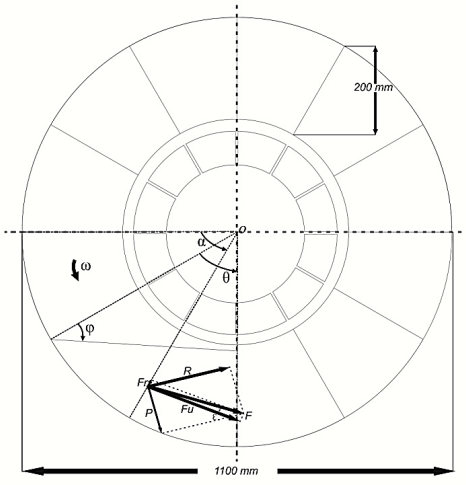

Figure 1. Force acting on the blade on the performance of the undershot water turbine.

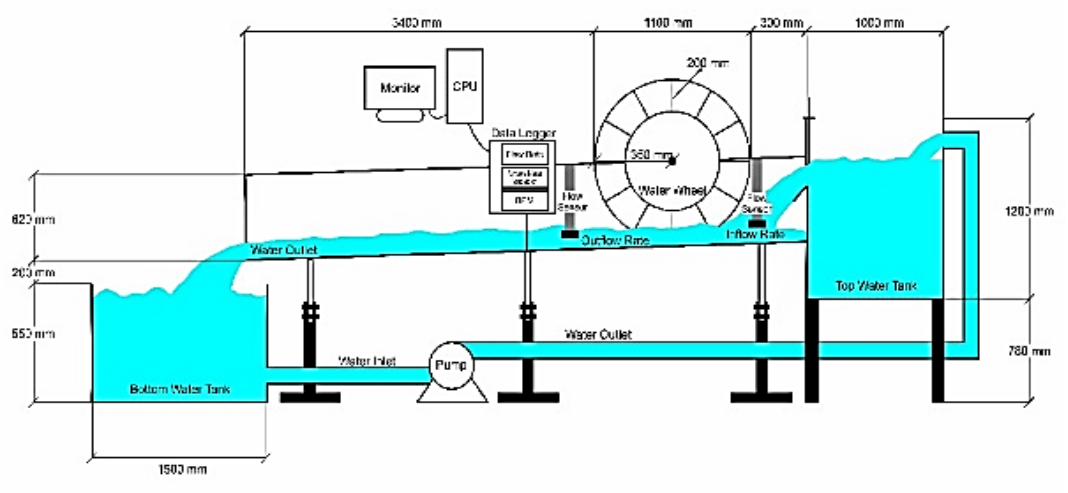

Figure 2. Diagram of the experimental setup.

3. Results and discussions

In this study, experimentation and assembly of tools were conducted in the alternative energy laboratory of ITN Malang. As shown in Figure 2. This test was conducted to determine the performance of the undershot type of waterwheel with a variety of materials used on the blade to obtain optimal performance. The blade consisted of four types of material, namely galvanized, aluminum, aluminum composite panel, and acrylic with different densities as shown in Table 1.

Table 1 shows the density of the material to be used for different blades. Galvanized material had the highest density of 7.49 g/cm^3, followed by the second-place aluminum which has a density of 2.71 g/cm^3, then followed by aluminum composite panel.

The fourth lowest material used for the blade has a density of 1.82 g/cm^3 which is owned by acrylic material. While the power used to turn the waterwheel was obtained from:

$$Pm : p.\ g.\ Q.\ H \tag{20}$$

Pm is the power of hydropower *P/Rho*is the density of water which has a value of 1000 kg/m^3, *g* is the earth's gravity has a constant of 9.8 m^2/s, for *Q* is the water discharge (m^3/mm)and H is the water level (m) which has a height of 0.5 m. After the calculation, the water horsepower achieved was 613.2 W which was used to rotate the waterwheel by varying the blades.

Figure 3 shows the density of the material with a waterwheel rotational speed with a 613.2 W water force. The largest rotation of waterwheel was owned by aluminum at 24 RPM with a density of 2.71 g/cm^3 while the lowest was the galvanizer at 20 RPM which has a density of 7.49 g/cm^3. From the experimental results, it was found that the difference between the four materials was due to different densities. There was an average trend seen that the greater the density used will affect the rotation of the waterwheel, which was the smaller the rotation. Meanwhile, with a small density, the rotation obtained at the waterwheel was getting bigger. This can be seen in the second place owned by acrylic which had 23 RPM speed and aluminum composite panel of 21 RPM which had a low average density.

Figure 4 shows the density of the waterwheel blade material and brake horsepower during the experiment. The first thing done was to find the torque of the undershot waterwheel. Torque is the power that the waterwheel must rotate because it is caused by the driving force of the moving water. To find out the brake horsepower, a simple rope brake-type dynamometer was used as shown in Figure 5.

This was a simple dynamometer consisting of two ropes wrapped around a drum whose water resistance would be measured using a measuring instrument. The loose side was connected to a measuring instrument to find out the pull that was symbolized by B. The right side of the rope bore the dead weight symbolized by A. The braking torque was obtained where A was the A scale, B was the B scale, and F was the force for power calculation.

Power : $T\ .\ W$

$$: (F.r)\ (2.\pi.n) \tag{21}$$

$$HP \quad : \frac{2.\pi.F.r.n}{550} Hp \tag{22}$$

: Lb. Ft.RPM
: 550 Ft.lb/s

No.	Material	Density [g/cm³]	Thickness [mm]	Water Horsepower [W]
1	Galvanized	7.49	0.98	613,.2
2	Aluminum	2.71	1.14	613.2
3	Aluminum Composite Panel	1.2	4	613.2
4	Acrylic	1.82	3	613.2

Table 1. Experimental results on water horsepower and density of water wheel blade material.

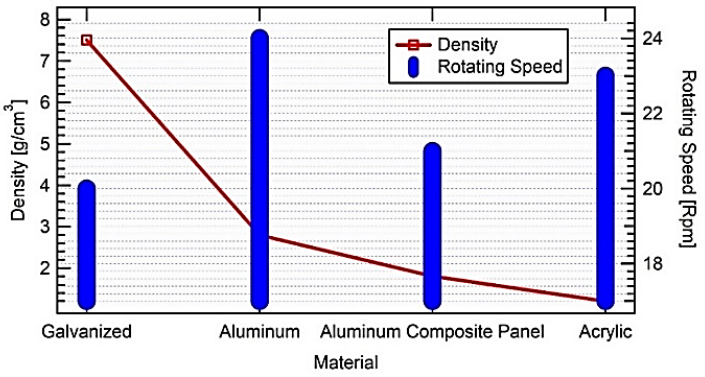

Figure 3. The density of the material at the rotational speed of the water wheel.

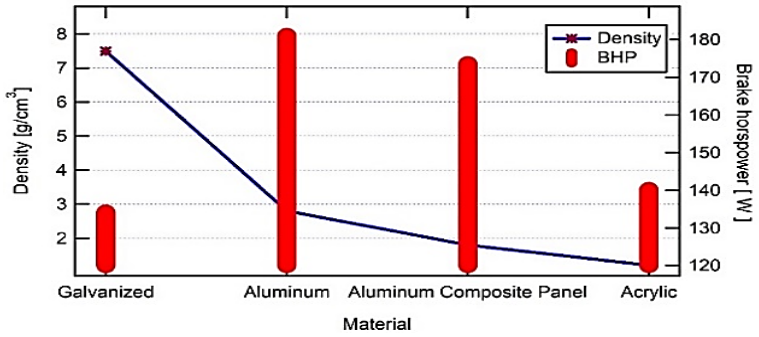

Figure 4. Density of material with horsepower brake.

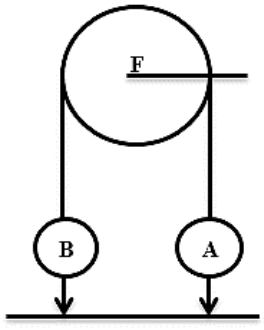

Figure 5. Rope brake dynamometer.

n is the RPM of the drum speed on the undershot wheel, *r* is the drum diameter with a diameter of 60 mm and *Δf* is the weight difference on the scale (lb). It can be seen in Figure 4 that the density of the material affected the brake horsepower obtained. The trend of the highest density started from galvanized and aluminum, followed by aluminum composite panels and acrylic. The brake horsepower produced by an undershot waterwheel using galvanized material was 134.1 W, while aluminum had a value of 181 W. These two materials had a difference of 46.9 W because the density of the material used was different, as aluminum. Acrylic material had 140.1 W brake horsepower value, while the aluminum composite panel had 173.5 W, a higher value than acrylic. Acrylic material and aluminum composite panel have a difference of 33.4 W. From the density of these two materials, the density value was not significantly far.

The density value on acrylic had a value of 1.2 g/cm^{3}and in the aluminum composite panel had 1.8 g/cm^3. The difference was 5 g/cm^3. This caused the brake horsepower value to differ in the two materials used, as from the whole materials, aluminum had the best result.

Figure 6 shows the efficiency of the undershot waterwheel and the efficiency of the undershot waterwheel. The left side graph showed the efficiency of the waterwheel which had the first trend up because the difference in density between aluminum materials had the highest value of 30%, while the lowest using acrylic material had an efficiency of 23%. The two materials used had a difference of 7% for micro hydro efficiency with a difference in value on the brake horsepower of 46.9 W. Aluminum in Figure 5 had the highest efficiency value, followed by aluminum composite panel which had an efficiency of 28% and acrylic material which had an efficiency of 23% had a difference of 4%. The efficiency of generator on the right side showed the highest generator efficiency using aluminum material with an efficiency of 4.2%, the second had an efficiency of 3.6% using the aluminum composite panel material and the third had the same efficiency of 3% using acrylic and galvanized materials. Aluminum had the highest efficiency because it had a density that was not that large compared to galvanized. In addition, the thickness of aluminum was very influential. Aluminum had a thickness of 1.14 mm thicker than galvanized which had 0.98 mm as shown in Table 1. The table also provided information about 3 mm thick acrylic which had the lowest micro hydro efficiency, while the aluminum composite panel material had a thickness of 4 mm. From Figure 5 and Table 1, it could be concluded that the higher density of the four materials used, the greater the efficiency. However, it must be accompanied by a thick material so that it had a large force as it affected the cross-sectional area when the pressure from the water and the torsion of the waterwheel increased.

4. Conclusion

This research designed and made a prototype of an undershot type of waterwheel which consisted of a waterwheel connected to a generator with the addition of a v-belt and pulley. The best results were obtained among the four materials used. Aluminum has the property of having a smaller material density which has a great efficiency, but it must be accompanied by the thickness of the material. By doing so, it had a large thrust force as it affected the cross-sectional area. When it was under pressure from water the torsion of the waterwheel increased. If the density is large but the thickness remains small, it will not increase the efficiency of the wheel like in galvanized material. Therefore, it is necessary to use some modifications to the waterwheel material to improve the performance of the system.

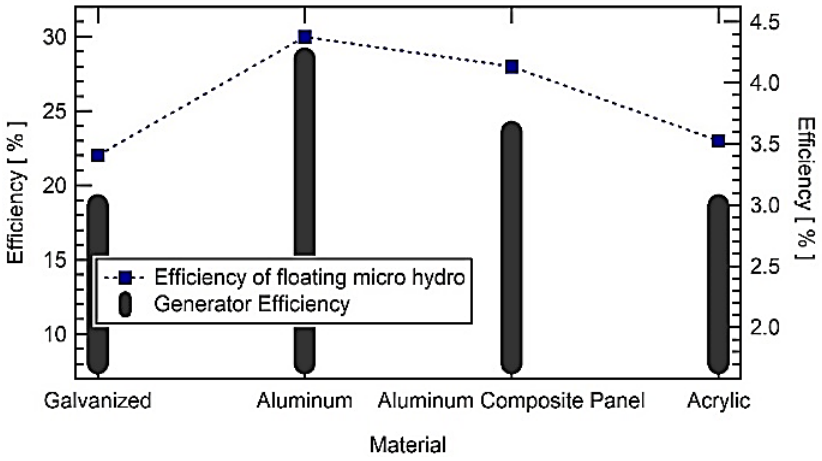

Figure 6. Efficiency of the waterwheel and generators.

Conflict of interest

The authors have no conflict of interest to declare.

Acknowledgments

The work described in this paper is supported by the National Institute of Technology Malang, Indonesia.

Funding

The authors received no specific funding for this work.

References

Adanta, D. (2020). The effect of channel slope angle on breastshot waterwheel turbine performance by numerical method. Energy Reports, 6, 606-610. https://doi.org/10.1016/j.egyr.2019.11.126

Agar, D., & Rasi, M. (2008). On the use of a laboratory-scale Pelton wheel water turbine in renewable energy education. *Renewable Energy*, *33*(7), 1517-1522. https://doi.org/10.1016/j.renene.2007.09.003

Denny, M. (2004). The efficiency of overshot and undershot waterwheels. *European journal of physics*, *25*(2), 193-202. https://doi.org/10.1088/0143-0807/25/2/006

Ishola, F. A., Azeta, J., Agbi, G., Olatunji, O. O., & Oyawale, F. (2019). Simulation for material selection for a Pico Pelton turbine's wheel and buckets. *Procedia Manufacturing*, *35*, 1172-1177. https://doi.org/10.1016/j.promfg.2019.06.073

Jain, S., Saini, R. P., & Kumar, A. (2010). CFD approach for prediction of efficiency of Francis turbine. In *The 8th International Conference on Hydraulic Efficiency Measurement*.

Kim, Y. T., Nam, S. H., Cho, Y. J., Hwang, Y. C., Choi, Y. D., Nam, C. D., & Lee, Y. H. (2009). Tubular-type hydroturbine performance for variable guide vane opening by CFD. In *New Trends in Fluid Mechanics Research: Proceedings of the Fifth International Conference on Fluid Mechanics (Shanghai, 2007)* (pp. 424-427). Springer Berlin Heidelberg. https://doi.org/10.1007/978-3-540-75995-9_139

Kumara, T. P. (2014). Analysis of floating type water wheel for pico hydro systems in Sri Lanka.

Müller, G., & Kauppert, K. (2004). Performance characteristics of water wheels. *Journal of Hydraulic Research*, *42*(5), 451-460. https://doi.org/10.1080/00221686.2004.9641215

Nuramal, A., Bismantolo, P., Date, A., Akbarzadeh, A., Mainil, A. K., & Suryono, A. F. (2017). Experimental study of screw turbine performance based on different angle of inclination. *Energy Procedia*, *110*, 8-13. https://doi.org/10.1016/j.egypro.2017.03.094

Nguyen, M. H., Jeong, H., & Yang, C. (2018). A study on flow fields and performance of water wheel turbine using experimental and numerical analyses. *Science China Technological Sciences*, *61*, 464-474. https://doi.org/10.1007/s11431-017-9146-9

Panwar, N. L., Kaushik, S. C., & Kothari, S. (2011). Role of renewable energy sources in environmental protection: A review. *Renewable and sustainable energy reviews*, *15*(3), 1513-1524. https://doi.org/10.1016/j.rser.2010.11.037

Prasad, V., Gahlot, V. K., & Krishnamachar, P. (2009). CFD approach for design optimization and validation for axial flow hydraulic turbine. Vol. 16, pp 229-236

Rohmer, J., Knittel, D., Sturtzer, G., Flieller, D., & Renaud, J. (2016). Modeling and experimental results of an Archimedes screw turbine. *Renewable energy*, *94*, 136-146. https://doi.org/10.1016/j.renene.2016.03.044

Setyawan, E. Y., Djiwo, S., & Sugiarto, T. (2017). Simulation Model Of Fluid Flow And Temperature Distribution In Porous Media Using Cylindrical, Convergent And Divergent Nozzles. *IJTS (International Journal Of Technology And Sciences)*, *1*(1), 1-10.

Setyawan, E. Y., Praswanto, D. H., Suwandono, P., & Siagian, P. (2019). Design of low flow undershot type water turbine. *Journal Of Science And Applied Engineering (JSAE)*, *2*(2).

Setyawan, E. Y., Djiwo, S., Praswanto, D. H., Suwandono, P., Siagian, P., & Naibaho, W. (2020). Simulation model of vertical water wheel performance flow. In *IOP Conference Series: Materials Science and Engineering* (Vol. 725, No. 1, p. 012020). IOP Publishing. https://doi.org/10.1088/1757-899X/725/1/012020

Sritram, P., Treedet, W., & Suntivarakorn, R. (2015). Effect of turbine materials on power generation efficiency from free water vortex hydro power plant. In *IOP Conference Series: Materials Science and Engineering* (Vol. 103, No. 1, p. 012018). IOP Publishing.

Sritram, P., & Suntivarakorn, R. (2017). Comparative study of small hydropower turbine efficiency at low head water. *Energy Procedia*, *138*, 646-650. https://doi.org/10.1016/j.egypro.2017.10.181

Suravut, S., Hirunlabh, J., Khedari, J., & Kiddee, K. (2017). Stand alone water wheel low speed surface aerator chaipattana rx-2-3, controller system. *Energy Procedia*, *138*, 751-755. https://doi.org/10.1016/j.egypro.2017.10.214

Vashisht, A. K. (2012). Current status of the traditional watermills of the Himalayan region and the need of technical improvements for increasing their energy efficiency. *Applied energy*, *98*, 307-315. https://doi.org/10.1016/j.apenergy.2012.03.042

Viollet, P. L. (2017). From the water wheel to turbines and hydroelectricity. Technological evolution and revolutions. *Comptes Rendus. Mécanique*, *345*(8), 570-580.

Wang, J. F., Piechna, J., & Müller, N. (2012). A novel design of composite water turbine using CFD. *Journal of Hydrodynamics, Ser. B*, *24*(1), 11-16. https://doi.org/10.1016/S1001-6058(11)60213-8

Williamson, S. J., Stark, B. H., & Booker, J. D. (2014). Low head pico hydro turbine selection using a multi-criteria analysis. *Renewable Energy*, *61*, 43-50. https://doi.org/10.1016/j.renene.2012.06.020

Yüksel, I. (2008). Hydropower in Turkey for a clean and sustainable energy future. *Renewable and Sustainable Energy Reviews*, *12*(6), 1622-1640. https://doi.org/10.1016/j.rser.2007.01.024

Yuksel, I. (2010). As a renewable energy hydropower for sustainable development in Turkey. *Renewable and Sustainable Energy Reviews*, *14*(9), 3213-3219. https://doi.org/10.1016/j.rser.2010.07.056

Yuksek, O., Komurcu, M. I., Yuksel, I., & Kaygusuz, K. (2006). The role of hydropower in meeting Turkey's electric energy demand. *Energy policy*, *34*(17), 3093-3103. https://doi.org/10.1016/j.enpol.2005.06.005